JOURNAL OF MATERIALS SCIENCE 32 (1997) 3355–3360

The nature of stresses in hot-filament chemical vapour deposited diamond thin films on WC substrates

S. CHATTERJEE, A. G. EDWARDS*, C. S. FEIGERLE*
*Department of Industrial Engineering and *Department of Chemistry, The University of Tennessee, Knoxville, TN 37996, USA*

The nature of film stresses in hot-filament chemical vapour deposited (HFCVD) diamond thin films on tungsten carbide substrates, is reported. Commercial WC substrates were subjected to various surface treatments. Subsequently, they were coated with a diamond film and examined for stresses using X-ray diffraction. All but one of the stress measurements indicated various levels of compressive stresses in the film and at the film–substrate interface. These stresses are compared with those obtained by other researchers. Intrinsic film stresses were also computed for diamond films and found to be tensile. WC drills, of 0.125 in. diameter, were also diamond coated and the stress levels measured along drill flanks and flutes. Significant variations were found in these stresses, and the results were analysed from a film–substrate adhesion perspective.

1. Introduction

Diamond thin films have numerous applications in optics, electronics, sensors, and manufacturing [1, 2]. Advances in these fundamental fields produce better technologies and lead ultimately to the development of new and improved applications. In the area of metal cutting, diamond thin films show significant promise not only because of their high hardness and refractoriness, but also due to their potential to coat complex surfaces. While thick films are used as brazed inserts, these films cannot be fabricated as drills, end-mills, or taps due to forming problems associated with the hardness and brittleness of diamond. Thus, a coating is an attractive alternative for such complex contours.

However, successful application of diamond-coated tooling to commercial metal cutting depends largely on the quality of film–substrate adhesion [3]. Adhesion of the film to the substrate is directly dependent on the film stresses present, and inappropriate or insufficient stresses may lead to film spalling in metal cutting applications.

All chemical vapour deposited (CVD) diamond films exhibit the presence of residual stresses, the majority of which are thermally induced. Additionally, variation in substrate grain sizes, film thickness, and film roughness can effect stress levels and adhesion strengths and lead to significant variabilities in cutting tool performance [4]. Suzuki *et al.* [5] state that few reports have adequately documented mechanical properties of WC–diamond composites, while Shen [4] notes the need for systematic studies of the interface type and stress levels for the development of diamond thin-film technology for complex contoured surfaces, such as drills and end mills.

Maintaining film-substrate adhesion is always a challenge in coated-tool fabrication and application. The adhesions and stresses of various ceramic coatings have been studied previously [6, 7]. However, in the area of diamond thin films on WC substrates, the source and fundamental nature of the stresses is not fully characterized and so not understood; thus, the motivation for undertaking this work.

Previous research in the area of diamond thin film stress and adhesion measurement is briefly reviewed and future trends and research issues are identified.

2. Review of previous research

Diamond films usually exhibit compressive stresses due to the relatively low thermal expansion coefficient of diamond as compared to common substrates. Drory [8] has stressed the importance of investigating such outstanding issues as mechanical characterization of diamond films, interface characterization, and development of suitable adhesion testing methods for diamond.

Kuo *et al.* [9] studied the adhesion of microwave plasma-deposited diamond films on WC (94.3% WC, 5.7%Co) using the indentation method. They used the slope dP/dX, of the load versus indentation length plot to assess the adhesion of the film. However, they did not report any stress measurements. In a similar study, Huang *et al.* [10] showed a dependence of adhesion strength on surface cobalt content of various cobalt-containing WC substrates. Indentation tests have also been used by other researchers to characterize the adhesion of CVD diamond to cobalt-free WC [11, 12] and Si (1 0 0) [13] substrates.

The tribological behaviour of CVD diamond thin films also plays an important role in their performance in machining and as wear-resistant coatings. Miyoshi [14] has demonstrated the use of tribology tests to assess friction and wear properties of diamond prepared by various methods. In general, the nature of the substrate must be properly characterized and understood when evaluating the tribological properties of CVD diamond films because the substrate characteristics affect the local bonding structure, impurities, and morphology of the film [15, 16]. Huang *et al.* [10] have observed significant differences in the coefficient of friction for diamond films grown on cemented WC substrates of various cobalt concentrations and grain sizes.

The stresses present in the film and at the film–substrate interface are expected to play a key role in determining the strength of a CVD diamond coating. While stresses in diamond films can be indirectly determined via the Raman shift [17, 18], X-ray diffraction (XRD) measurements can be used to compute film stresses directly. Choi *et al.* [19] have used XRD techniques to study the dependence of stresses, in CVD diamond films on Si (1 0 0). We are unaware of any similar study for CVD diamond on cemented WC substrates. Here proper surface pretreatment is critical for successful deposition of diamond and is expected strongly to affect the forces at the interface. In this study, XRD analysis was used to measure the stress at the surface of the WC prior to deposition and at the interface following CVD diamond film coating. The stresses in the diamond film, measured by Raman and XRD, have also been compared.

3. Experimental procedure

3.1. Sample specifications and preparation

The samples were: (i) cylindrical rods, 0.25 in. (~ 0.64 cm) diameter and 0.5 in. (~ 1.27 cm) long, 94% WC and 6% Co with a grain size of $(32.0\text{–}40.0) \times 10^{-6}$ in. (0.8–1.0 μm); (ii) commercially available WC drills, 0.125 in. (~ 0.32 cm) diameter, 118° point angle and 25° helix angle with the same composition as (i). The as-received cylindrical rods were ground with a 220 grit diamond wheel and polished. They were then ultrasonically cleaned in reagent-grade acetone to remove surface organics.

Three different surface preparation methods were used to clean the surface of the rods and remove surface cobalt. In the first method the samples were only ultrasonically cleaned with acetone. In the second method, labelled the nitric acid (NA) treatment, an acetone-treated sample was ultrasonically treated with a 1:1 vol/vol mixture of $HNO_3 + H_2O$ for 15 min, rinsed with 18 Ω water and sonicated again in 18 Ω water for 5 min. Finally, the sample was sonicated first in acetone and then in methanol to remove any surface organics. This method was also used to prepare the drills for diamond deposition. The third method was a proprietary chemical treatment (labelled PT) for surface cobalt removal [20]. These samples were also sonicated in acetone and then in methanol.

3.2 Diamond deposition conditions

Diamond films were deposited using HFCVD in a reactor constructed from a high-vaccum six-way cross. The arrangement for the depositions is shown in Fig. 1. Growths were performed with a 1% methane–hydrogen gaseous mixture at a 100 standard $cm^3\,min^{-1}$ flow rate, 38–40 torr (1 torr = 133.322 Pa) chamber pressure for rods and 15 torr for drills, and substrate and filament temperatures of 1050 and 2120 K, respectively. Substrate and filament temperatures were measured with a disappearing filament optical pyrometer and are reported without correction for emissivity.

3.3. Raman spectroscopy

The diamond films were analysed using a Dilor XY Raman spectrometer with a microscope attachment and CCD detector. Spectra were recorded using 100 mW of 514.5 nm excitation focused on the samples through the mag × 80 objective of the microscope. No degradation of the samples was observed under these conditions. The Raman shifts reported in this paper are based upon calibrating the instrument using the 1332.2 cm^{-1} line from a single-crystal diamond sample.

3.4. XRD conditions

The films were step-scanned on WC [1 0 2] and diamond [1 1 1] with a chromium radiation of 0.22897 nm wavelength. A rectangular collimator of 5 mm aperture was used during scanning. The residual stresses were automatically calculated from the scans.

4. Results and discussion

4.1 Raman analysis

A typical Raman spectrum is shown in Fig. 2. The band in this figure indicates a fairly high-quality diamond film. One indicator of film quality is the relative intensity of the diamond band to non-diamond band which appears between 1500 and

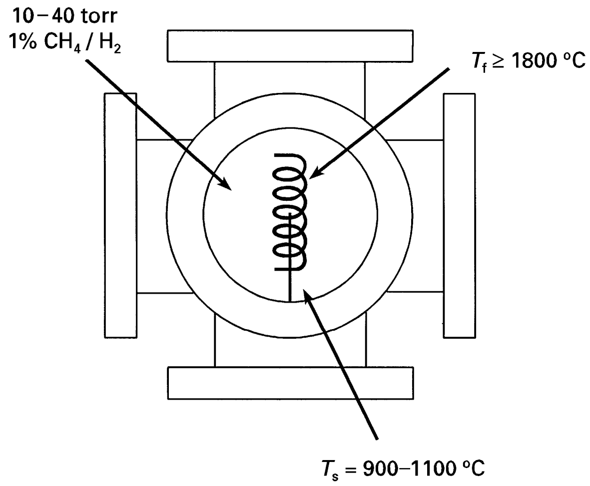

Figure 1 Schematic diagram of the CVD configuration.

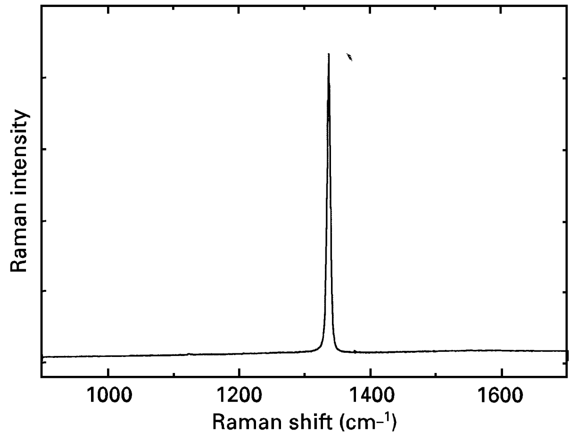

Figure 2 A typical Raman shift for the diamond film.

1600 cm^{-1}. A careful examination of Fig. 2 shows only a slight deviation in the baseline in the non-diamond region.

The observed Raman shifts are tabulated below. In Table I the treatments are referred to as NA (nitric acid), and PT (proprietary treatment). In addition, "scratch" refers to scratching half of a sample with a diamond paste to enhance diamond nucleation. The shift in the Raman peak position is relative to that of natural diamond peak at 1332.2 cm^{-1}.

A positive shift in the band centre is explained due to the presence of compressive stresses in the film [17, 21]. The magnitude of this stress has been determined by applying the pressure coefficient of 0.237 cm^{-1} $Kbar^{-1}$, obtained by others from measurements on diamond anvil [22]. The data in Table I indicate that scratching the rod with diamond paste does not improve the film quality. Scratching smooth silicon surfaces for enhanced diamond nucleation is well known. The WC substrates used here possessed a relatively coarse topography. Thus, further scratching of these surfaces may not be necessary. There is also a noticeable difference in the Raman shifts for the two treatments used on the drills. Why this happens is unknown at this time.

All films in this study exhibited a compressive stress state. The effects of the surface preparation methods on the pre-deposition surface topography and resultant film quality have been reported earlier [23]. From the data in Table I it may be inferred that the net effect of the entire process affects film stresses and ultimately, film adhesion.

4.2. X-ray analysis of stresses in cylindrical rods

The determination of stresses by XRD is based on established elasticity theory. In the presence of two-dimensional stresses in the plane of the film, with zero normal stress, the strain in the (ϕ, ψ) direction is given as

$$\varepsilon_{(\phi,\psi)} = (d_\psi + d_0)/d_0 = (a_\psi - a_0)/a_0 \quad (1)$$

where d_0 and a_0 are the unstressed atomic planar spacing and lattice parameters, respectively, and d_ψ and a_ψ correspond to those for the stressed condition in a plane perpendicular to the direction (ϕ, ψ). Here, ϕ is the resultant two-dimensional stress direction and ψ is the tilt of the sample surface with respect to the incident X-ray beam. From elasticity theory, the stress, σ_ϕ, in the resultant direction and the strain are related by

$$\varepsilon_{(\phi,\psi)} = (1 + \nu)\,\sigma_\phi \sin^2 \psi/E - \nu(\sigma_1 + \sigma_2)/E \quad (2)$$

where ν is Poisson's ratio, E is the Young's modulus, and $\sigma_\phi = \sigma_1 \cos^2 \phi + \sigma_2 \sin^2 \phi$ is the stress in the surface of the coating. Thus

$$(d_\psi - d_0)/d_0 = (1 + \nu)\,\sigma_\phi \sin^2 \psi/E - \nu(\sigma_1 + \sigma_2)/E \quad (3)$$

From these equations, a straight-line plot of $\varepsilon_{(\phi,\psi)}$ as a function of $\sin^2 \psi$ at constant ϕ has a slope related to σ, the stress; the elastic constants and the lattice parameters in the stress-free condition, can be derived and plotted.

Thus, the lattice parameter will be related to $\sin^2 \psi$ and this is the well-known "$\sin^2 \psi$" for relating the lattice parameter, internal stresses, and ψ [24].

Fig. 3a and b show the *d*-spacing and intensity and FWHM versus $\sin^2 \psi$ plot obtained by scanning the diamond [1 1 1] of a CVD-coated WC rod with NA treatment. The non-linear and undulating *d*-spacing plot indicates fairly large grain sizes and preferred orientation. The variation of integrated intensity with ψ confirms a preferred orientation. The small FWHM bands indicate film crystallinity.

TABLE I Raman analysis

Sample	Treatment	Position (cm^{-1})	Shift (cm^{-1})	Stresss (GPa)
A	NA	1136.9	4.7	− 2.0
A	PT	1337.0	4.8	− 2.0
A	PT	1338.5	6.3	− 2.7
	Scratch	1338.5	6.3	− 2.7
Drill	NA	1335.2	3.0	− 1.27
Drill	PT	1333.7	1.3	− 0.55

4.3. Interface stresses

XRD analysis of WC diffractions was performed to investigate the dependence of the interface stresses on substrate preparation and diamond deposition. Fig. 4 shows the stress levels measured by scanning the WC [1 0 2] for various sample treatments and depositions. Two of these were for samples which were treated but were not subject to HFCVD diamond deposition, whereas the other three were both treated, and deposited with diamond. It is clear that the acetone cleaning treatment exhibited maximum stresses with the largest variations, whereas the nitric acid-treated HFCVD diamond-WC composite had minimum stresses. The proprietary treatments, with or without the films, possessed intermediate stress values.

It is well-known that any machining process leaves the machined surface in a compressive stress state [25]. Thus, the initial surface preparation by grinding leaves a fairly high compressive stress on the WC

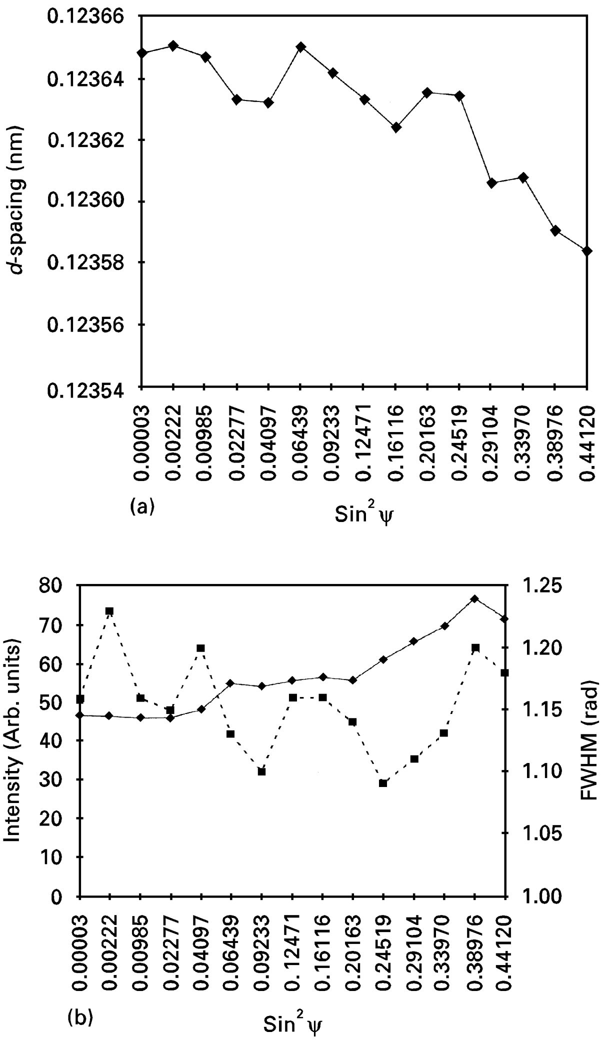

Figure 3 (a) d-spacing versus $\sin^2\psi$ for diamond on WC rods. (b) (◆) Intensity versus $\sin^2\psi$ for diamond on WC rods; (■) FWHM.

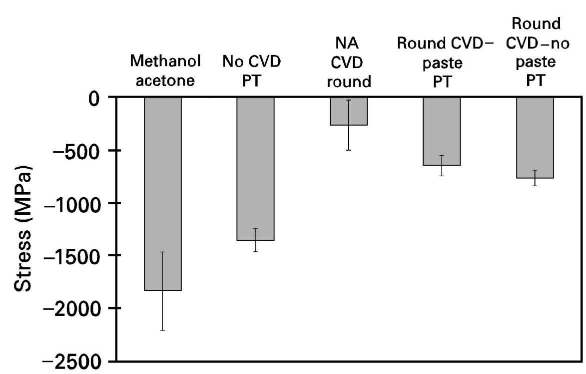

Figure 4 Film stresses for the WC rods.

substrate. As the acetone treatment only cleans the surface, the measured stress is attributed directly to grinding. The PT treatment, on the other hand, relieves some of the stresses by the chemical removal of the cobalt from the substrate. The removal of cobalt creates voids in the surface [23] and some stress relaxation may occur due to this. When the substrates are coated the annealing effect of the high deposition temperature results in significant reduction of the compressive stresses. This is clearly seen from the stress values obtained.

The drop in surface stress values with HFCVD of diamond raises the question of appropriate levels of initial compressive stresses. If the WC is to be used as a cutting tool, it is desirable that the film–substrate composite be in compression for efficient machining. It may, therefore, be appropriate to perform a systematic study to determine whether relationships exist between initial grinding-induced compressive levels and diamond-coated tool performance. The additional finding from Fig. 4 is a comparatively larger drop in stresses for the nitric acid treatment. Although Huang *et al.* [10] claim improved tool life of nitric acid-etched diamond-coated inserts, this study suggests that a detailed study relating surface preparation methods, substrate grain size, deposition parameters, work material properties, and machining parameters is needed to understand truly the effect of surface preparation on the film stress levels and machining performance.

4.4. Intrinsic film stresses in the cylindrical rods

The total measured stresses in a film are the sum of thermal and intrinsic stresses, or

$$\sigma_{\text{total}} = \sigma_{\text{thermal}} + \sigma_{\text{intrinsic}} \qquad (4)$$

The thermal stresses originate from the thermal expansion coefficient differences between the film and substrate. The intrinsic stresses are due to ingrown defects from the growth process or from structural mismatch between film and substrate. XRD of diamond is used to study the total stresses. The stresses measured based on diamond diffraction tend to be significantly larger than those based on WC, presumably, due to the effects of ingrown defects in the diamond film and the larger thermal stresses.

The thermal stress is given by

$$\sigma_{\text{thermal}} = E_{\text{film}}\,(\alpha_s - \alpha_f)\,\delta T/(1 - \nu_f) \qquad (5)$$

where E_{film} is the Young's modulus of the film, α_s and α_f are the substrate and film thermal expansion coefficients, respectively. δT is the difference between the deposition temperature and the room temperature at which the stresses are measured, and ν_f is Poisson's ratio for the film. The values of σ_{thermal} for this study were calculated using the following values for the above parameters: $E_{\text{film}} = 1.034 \times 10^{12}$ Pa for diamond [26], $\alpha_s = 5.5 \times 10^{-6}$ K^{1} [27], $\alpha_f = 1.5 \times 10^{-6}$ K^{-1} [26], $\delta T = 763.5$ and 740.65 K for the proprietary and nitric acid-treated samples, and $\nu_f = 0.16$. The intrinsic stresses were determined as the difference between the measured total and calculated thermal stresses.

Fig. 5 shows the thermal, intrinsic, and total stresses for cylindrical rods for the diamond [1 1 1] scan for the proprietary (PT) and nitric acid (NA) treatments. All intrinsic stresses are observed to be tensile in nature and agree with the results of Choi *et al.* [19]. However, it should be noted that their measurements are based on diamond [2 2 0] diffraction grown on a

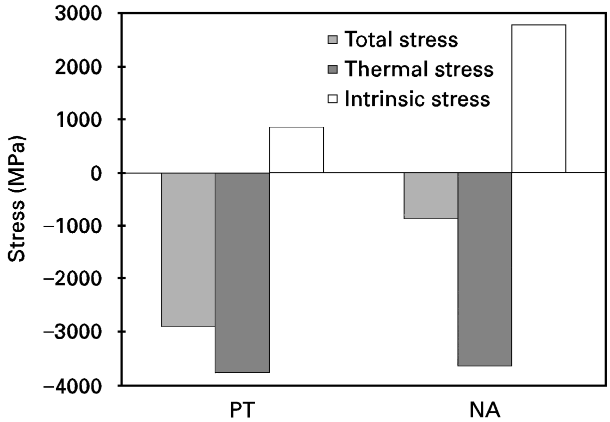

Figure 5 Total and intrinsic stresses.

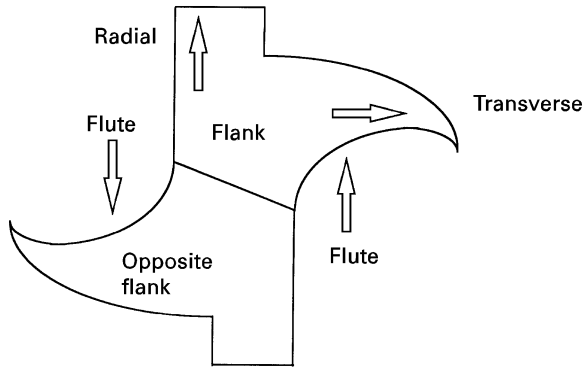

Figure 6 Schematic diagram of drill measurement points.

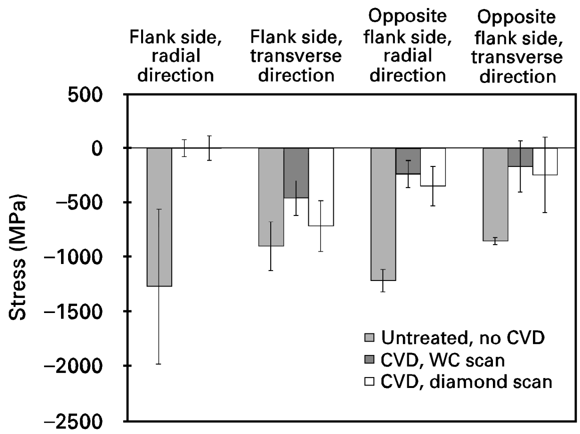

Figure 7 Radial and transverse film stresses on drills.

Si [1 0 0] substrate under different growth conditions. A comparison of these stress values with those for sample A (NA and PT treatments) using diamond anvil measurement constants [22] in Table I, indicates a significant difference between the XRD-measured total stress (−873 MPa) and the diamond anvil method (−2.0 GPa) for the NA treatment. For the PT treatment, this variation is smaller at −2900 MPa for the XRD measurement and (−2.0–2.7 GPa) for the diamond anvil method.

As compressive stresses in diamond films are desirable from a machining perspective, increased levels of compressive stresses may be obtained from decreased levels of intrinsic stresses or increased levels of thermal stresses. It is clear from the above thermal stress equation the δT is the only parameter that may be altered to increase thermal stresses. However, this may be difficult because of extreme sensitivity of diamond growth to the deposition temperature. It may be possible to start with higher levels of pre-deposition stress on the substrates such that desirable levels of stresses remain after stress relaxation due to deposition and intrinsic stress effects. A designed experimentation may be useful in relating tool life to pre-deposition stress levels, growth conditions, and post-deposition stresses.

4.5. Stresses in drills

Both interface and film stresses were measured for drills without treatment or growth and after NA treatment and diamond deposition. A schematic diagram of the stress measurement points on the drill is shown in Fig. 6. The drills were scanned for both WC and diamond diffracting planes. This was done as a part of a qualification process for the coated and uncoated drills for use in subsequent machining tests. The results of the machining tests will be published elsewhere. An examination of the stress levels in Fig. 7 demonstrates stress imbalances between the radial and transverse directions attributable to the drill manufacturing process.

The stresses in the deposited drills, seen in Fig. 7, were all compressive except one, where it was slightly tensile. The stress levels for the coated drills are seen to be lower than the uncoated ones. This may be explained as the stress relaxation effects of the high deposition temperatures. Variations in stress levels can be observed between the cutting edges. Also, the stresses are different for the diamond film and WC with the film showing higher stresses. This is expected because of diamond's lower expansion coefficient. Thus, the compressive stresses increase from the substrate to the film and vary significantly for the samples tested.

The geometry effect on stresses can be seen by comparing Figs 5 and 7 for the diamond scan. The film stresses for the drills are significantly lower than those for the rods. The reasons for this are unknown at this time.

Stresses in the rake face (flute) were also measured. Fig. 8 shows these stresses for as-is versus CVD growths. Again, stresses are seen to vary and post-CVD stresses range from slightly tensile to compressive. Also, the values are different from those of the flank surface stresses noted in Fig. 7.

The implications of the stress variabilities are related to the performance of the drills during drilling. If stresses are tensile, then an earlier advent of film spalling is likely. Also, significant variations in the stress levels will affect the adhesion of the film to the substrate due to the nature of the drill geometry with inherent stress concentrations at the edges and the tip. This effect will be further complicated by the rise in temperature. Although diamond has excellent refractoriness, the original stress variations may lead to

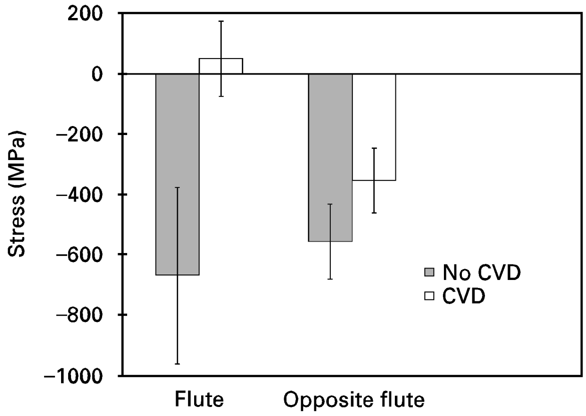

Figure 8 Flute stresses on the drill.

increased stress fluctuations at the interface during cutting with premature tool failure through film spalling. Coupled with this is the edge effect, that is, the nature of the edge deformities in forms of machining gouges or marks from the drill manufacturing process. The extent of these imperfections may determine film nucleation, further growth, and adhesion. Whether this actually happens for diamond-coated drills is unknown at this time and is a topic for future research.

The issue of determining appropriate processing parameters for acceptable levels of stress variation is also important. In other words, what are acceptable bounds of stress variations for given applications or film failure criteria and how can the deposition process be controlled to yield films within those bounds? An additional question is the dependence of stresses on film thickness and substrate grain size. Although some reports stress the importance of reducing variability of performance starting with the raw material and processing and deposition conditions [4, 8], extensive investigations are yet to be seen [28].

5. Conclusion

This study examined the stress levels of diamond thin films deposited on WC cylinders and drills. Significant stress variations were observed from the measurements and revealed preferred orientations, relatively smooth surfaces, and stress gradients. All but one of the stresses for the drills were compressive. This study underscores the need for further research in the following areas:

(a) the extent of allowable stress variations for acceptable cutting tool performance;

(b) the effect of cutting edge imperfections on film nucleation, further growth, and adhesion;

(c) the dependence of surface preparation methods, substrate grain size, deposition parameters, work material properties, and machining parameters on machining performance; and

(d) geometry effects of tools, such as taps and end mills, on films stresses.

Acknowledgements

The authors gratefully acknowledge the financial support for this research from the Center for Material Processing, The University of Tennessee, Knoxville, and the National Science Foundation (grant CTS-9202575). The authors thank CARMET, Duncan SC, for the WC rods, SP^{3}Inc., Mountain View, CA, for surface treatment of the samples, and TEC, Knoxville, particularly, B. Pardue and S. Fitch, for the measurement of stresses.

References

1. F. MASON, *Am. Machinist* February (1990) 43.
2. P. K. BACHMANN and R. MESSIER, *C&EN* May **15** (1989) 24.
3. H. E. HINTERMANN and A. K. CHATTOPADHYAY, *Ann CIRP* **42** (1993) 769.
4. C-H SHEN, in "Applications of Diamond Films and Related Materials: Third International Conference", edited by A. Feldman, Y. Tzeng, W. A. Yarbrough, M. Yoshikawa and M. Murakawa (Washington, 1995) p. 175.
5. T. SUZUKI, T. HATTORI, A. ENDO, M. YAGI, K. SHIBUKI and M. KOBAYASHI, *ibid.*, p. 927.
6. A. J. PERRY, *Thin Solid Films* **81** (1981) 357.
7. D. S. RICKERBY, *J. Vac. Sci. Technol.* **4** (1986) 2809.
8. M. D. DRORY, in "Applications of Diamond Films and Related Materials: Third International Conference", edited by A. Feldman, Y. Tzeng, W. A. Yarbrough, M. Yoshikawa and M. Murakawa (Washington, 1995) p. 313.
9. C.-T. KUO, T-Y. YEN and T.-H. HUANG, *J. Mater. Res.* **5** (1990) 2515.
10. T. H. HUANG, C.-T. KUO and T. S. LIN, *Surf. Coat. Technol.* **56** (1993) 105.
11. K. SAIJO, M. YAGI, K. SHIBUKI and S. TAKATSU, *ibid.* **43**/**44** (1990) 30.
12. S. TAKATSU, K. SAIJO, M. YAGI and K. SHIBUKI, *Mater. Sci. Eng.* **A140** (1991) 747.
13. D. E. PEEBLES and L. E. POPE, *J. Mater. Res.* **5** (1990) 2589.
14. K. MIYOSHI, in "Applications of Diamond Films and Related Materials: Third International Conference", edited by A. Feldman, Y. Tzeng, W. A. Yarbrough, M. Yoshikawa and M. Murakawa (Washington, 1995) p. 493.
15. S. S. PERRY, J. W. AGER III and G. A. SOMORJAI, *J. Mater. Res.* **8** (1993) 2577.
16. M. N. GARDOS and B. L. SOCIANO, *ibid.* **5** (1990) 2599.
17. D. S. KNIGHT and W. B. WHITE, *ibid.* **4** (1989) 385.
18. M. YOSHIKAWA, G. KATAGIRI, H. ISHIDA, A. ISHITANI, M. ONO and K. MATSUMURA, *Appl. Phys. Lett.* **55** (1989) 2608.
19. S. K. CHOI, D. Y. JUNG and H. M. CHOI, *J. Vac. Sci. Technol.* **A14** (1996) 165.5.
20. Sp^3 Inc., Mountain View, CA.
21. S. R. SAILS, D. J. GARDINER, M. BOWDEN, J. SAVAGE and S. HAQ, *Appl. Phys. Lett.* **65** (1994) 43.
22. S. K. SHARMA, H. K. MAO, P. M. BELL and J. A. XU, *J. Raman Spectrosc.* **16** (1985) 351.
23. S. CHATTERJEE, A. G. EDWARDS, A. NICHOLS and C. S. FEIGERLE, *J. Mater. Sci.* (1996) accepted.
24. B. D. CULLITY, "Elements of X-Ray Diffraction" (Addison-Wesley, NY, 1959).
25. A. BHATTACHARYA, "Metal Cutting - Theory and Practice" (Central Book Publishers, Calcutta, 1984).
26. K. E. SPEAR, *J. Am. Ceram. Soc.* **72** (1989) 171.
27. J. L. HUNT and A. T. SANTHANAM, in "Proceedings of the ASME Winter Annual Meeting", edited by B. Klamecki, Dallas, PED Vol. 43 (The American Society of Mechanical Engineers, NY, 1990) p. 139.
28. *R and D Mag* June (1996) 42.

Received 13 September and accepted 30 October 1996